# Simultaneous suppression of multiple programmed cell death pathways by microRNA-105 in cardiac ischemic injury

Sunhye Shin

The Graduate School

Yonsei University

Department of Integrated OMICS for

Biomedical Science

# Simultaneous suppression of multiple programmed cell death pathways by microRNA-105 in cardiac ischemic injury

Directed by Professor Gyoon Hee Han

The Master's Thesis
Submitted to the Department of Integrated OMICS for Biomedical Science,
the Graduate School of Yonsei University
in partial fulfillment of the
requirements for the degree of
Master of Biomedical Science

Sunhye Shin

December 2017

연세대학교
YONSEI UNIVERSITY

This certifies that the Master's Thesis
of Sunhye Shin is approved.

Thesis Supervisor: Gyoon Hee Han

Thesis Committee Member#1: Nam-On Ku

Thesis Committee Member#2: Ki-Chul Hwang

The Graduate School

Yonsei University

December 2017

# Acknowledgements

First and above all, I would like to deeply thank my father God.
Must your name be exalted, honored, and glorified.

I want to thank Prof. Gyoon Hee Han, Prof. Nam-on Ku for their guidance and especially appreciate to Prof. Ki-Chul Hwang for his support to make my experience productive.

Dr. Sang Woo Kim, I deeply thank to his advice, encouragement and support. I couldn't have finished this work without his help.
In addition, I also thank Seahyoung Lee, Soyeon Lim, Jung-Won Choi, Chang Youn Lee, Jiyun Lee, Hyang-Hee Seo, ByeongWook Song, Jun-Hee Park, Il-kwon kim who helped me for accomplishing this.

I would like to express my sincere thanks to my family for all their unconditional love.

I'll not forget your support and love.

Thank you.

December, 2017
Sunhye Shin

# TABLE OF CONTENTS

# LIST OF FIGURES

**ABSTRACT**

# Simultaneous suppression of multiple programmed cell death pathways by microRNA-105 in cardiac ischemic injury

Shin, Sunhye

*Department of Integrated OMICS for Biomedical Science*

*The Graduate School, Yonsei University*

(Directed by Professor Gyoon Hee Han)

Recent studies have shown that several upstream signaling elements of apoptosis and necroptosis are closely associated with acute injury in the heart. In our study, we observed that miR-105 was notably dysregulated in rat hearts with myocardial infarction (MI). Thus, the purpose of this study was to test the hypothesis that miR-105 participates in the regulation of RIP3/p-MLKL- and BNIP3-dependent necroptosis/apoptosis in H9c2 cells and MI rat hearts. Our

results show that the RIP3/p-MLKL necroptotic pathway and BNIP3-dependent apoptosis signaling are enhanced in H9c2 cells under hypoxic conditions, whereas compared with these pathways in the controls, those in miR-105-treated H9c2 cells are suppressed. Mechanistically, we identified miR-105 as the miRNA directly suppressing the expression of RIP3 and BNIP3, two important mediators involved in cell necroptosis and apoptosis. Furthermore, MI rat hearts injected with miR-105 had decreased infarct sizes, indicating that miR-105 is among three miRNAs that function simultaneously to suppress necroptotic/apoptotic cell death pathways and to inhibit MI-induced cardiomyocyte cell death at multiple levels. Taken together, miR-105 may constitute a new therapeutic agent for the treatment of ischemic heart disease.

---

Key words: Apoptosis, ischemic heart, microRNA-105, necroptosis

# Simultaneous suppression of multiple programmed cell death pathways by microRNA-105 in cardiac ischemic injury

Shin, Sunhye

*Department of Integrated OMICS for Biomedical Science*

*The Graduate School, Yonsei University*

(Directed by Professor Gyoon Hee Han)

## I. INTRODUCTION

Heart disease, including heart failure, myocardial infarction (MI) and ischemia reperfusion (I/R), is one of the causes of mortality and morbidity worldwide [1-4]. Numerous studies have demonstrated that MI and I/R injuries lead to various types of cardiomyocyte cell death (necrosis, apoptosis and

autophagy) [5, 6]. For many years, apoptosis was considered the only form of regulated cell death, according to studies investigating myocyte cell death; apoptosis is a well-established programmed form of cell death that can be initiated by a mitochondrial-mediated intrinsic pathway and death receptor-mediated extrinsic pathway [5, 7]. However, necrosis has been described as an 'unregulated' or 'accidental' form of cell death. Many studies have focused on blocking apoptosis because it was considered the only form of regulated cell death. However, recent advances have demonstrated that both apoptosis and necrosis can be regulated in various types of cell death [8-11]. Necroptosis is another regulated cell death mechanism that exists in various diseases, including MI, I/R injury, heart failure, and inflammation [11, 12], and it is regulated by the necrosome, which consists of receptor-interacting protein kinase 3 (RIP3) and mixed lineage kinase-like (MLKL) [9]. Mechanistically, the initiation of necroptosis is triggered by death ligands, such as tumor necrosis factor (TNF)-α, TNF-related apoptosis inducing ligand (TRAIL), and pathogen-associated molecular patterns (PAMPs) [10].

In particular, RIP3 is a key molecule that protects the ischemic heart and improves cardiac function after ischemia- and oxidative stress-induced myocardial necroptosis [13]. Several studies have shown that RIP3 is involved in

reactive oxygen species (ROS) production by mitochondria under high glucose-induced injury and inflammation in H9c2 cardiac cells [14, 15]. Moreover, BCL2/adenovirus E1B 19 kDa protein-interacting protein 3 (BNIP3) is a well-known pro-apoptotic protein under hypoxic and ischemic conditions. BNIP3 promotes the apoptosis, necrosis and autophagy of cardiomyocytes in disease states [16-18]. Cardiomyocyte cell death due to high BNIP3 expression leads to mitochondrial permeability transition pore (MPTP) opening, mitochondrial swelling, and outer mitochondrial membrane (OMM) rupture by the release of cytochrome c [16]. The disruption of BNIP3 inhibits apoptosis, is crucial for ischemic cardiomyocytes, and is important for cardiac cell survival [16-20]. We also reported that downregulating BNIP3 is an effective means to prevent cardiac cell death [21]. Nevertheless, inhibition of necroptosis or apoptosis remains limited as a therapeutic treatment in heart disease. However, recent studies have suggested a new strategy that combines targets of both necroptosis and apoptosis [22, 23].

MicroRNAs (miRNA), endogenous, 22-nucleotide-long, small non-coding RNAs, control gene expression by targeting mRNAs [24]. Moreover, miRNAs regulate the expression of multiple genes by binding to target transcripts through imperfect sequence complementarity. The capacity of miRNAs to target multiple genes makes them useful therapeutic tools that can be more potent than agents

that act on a single gene. miRNAs are known to play important roles in pathological conditions involving multiple cell death pathways, including MI and heart failure. Recent studies have found that miRNAs regulate apoptosis, autophagy, and necroptosis by targeting key regulators under pathophysiological conditions [25]. Furthermore, synergistic interactions of miRNAs can increase the efficacy of therapeutics while reducing their side effects and slowing the development of drug resistance [26].

In this report, we identified miR-105, a new miRNA that targets RIP3 and BNIP3. Moreover, we demonstrate that miR-105 activation may potentially offer a therapeutic approach to prevent myocardial cell death by inhibiting apoptosis and necroptosis in MI.

## II. MATERIALS AND METHODS

### 1. Materials

H9c2 cells were obtained from the Seoul Korean Cell Line Bank (Seoul, Korea). Dulbecco's modified Eagle's medium (DMEM) and penicillin-streptomycin were obtained from Thermo Fisher Scientific (Thermo Fisher Scientific, Waltham, Massachusetts, USA). Fetal bovine serum (FBS) was obtained from Atlas Biologicals (Atlas Biologicals, Colorado, USA) for H9c2 cell culture. Primary antibodies were used for immunoblot assays: RIP3 (sc-374639, Santa Cruz Biotechnology, Texas, USA), MLKL (sc-293201, Santa Cruz Biotechnology), p-MLKL (ab196436, Abcam, Cambridge, UK), BNIP3 (ab10433, Abcam), BAX (ab32503, Abcam), caspase 3 (AB3623, Millipore, Massachusetts, USA), BAK (#12105S, Cell Signaling Technology, Massachusetts, USA), TNF-R1 (sc-8436, Santa Cruz Biotechnology) and TLR 4 (NB100-56566, Novus Biologicals, Colorado, USA). Horseradish peroxidase (HRP)-conjugated anti-mouse IgG, anti-goat IgG, and anti-rabbit IgG were obtained from Santa Cruz Biotechnology.

### 2. Animal experiments and histological analysis

All experimental procedures for animal studies were approved by the

Committee for the Care and Use of Laboratory Animals of Catholic Kwandong University College of Medicine (CKU01-2017- 002) and performed in accordance with the Committee's Guidelines and Regulations for Animal Care. Seven-week-old male Sprague-Dawley rats (220 ± 30 g) were used for the MI model and were anesthetized via intraperitoneal injection of Zoletil (30 mg/kg) and xylazine (10 mg/kg). Rats were ventilated via the trachea using a ventilator (Harvard Apparatus, Holliston, MA, USA) and then were subjected to a median sternotomy. MI was induced by a tightened ligation of the left anterior descending coronary artery using a 7-0 Prolene suture (Covidien, Dublin, Ireland) for 1 h, 24 h, or 48 h. To obtain cardiac tissue, we perfused hearts with PBS and fixed them with 4% formaldehyde. After paraffin embedding, sections were cut at a thickness of 3 mm. For analysis of target protein expression patterns in rat hearts under pathological conditions, tissue slides were blocked with blocking solution [2% normal horse serum, 1% bovine serum albumin (BSA), 0.1% Triton X-100 and 0.05% Tween 20 in PBS] for 20 min and then incubated with a mixture of two primary antibodies in dilution buffer (1% BSA in PBS) overnight at 4 °C. Slides were rinsed in PBS and incubated in a mixture of two fluorescence-conjugated secondary antibodies in the dark for 1 h. The expression of target protein was observed by virtual microscopy (BX51/dot slide; Olympus, Tokyo, Japan).

### 3. Infarction size analysis and cell death assays of heart tissues

To measure myocardial infarct size, hearts were perfused with 1% 2,3,5-triphenyltetrazolium chloride (TTC) (Sigma, St Louis, MO) for 1 h at 37 °C and incubated in 4% formaldehyde overnight at 4 °C. The heart sections were photographed with a digital camera. The area stained by TTC was identified as viable myocardium (deep red). The infarcted area was identified as the area not stained by TTC (yellow-white). The infarcted area was measured directly by planimetry of normal and infarcted left ventricular myocardia using ImageJ software. In infarcted hearts, apoptotic and necrotic cells were determined using PI and TUNEL staining. All PI-positive cells indicated necrotic cell death, and TUNEL only positive cells indicated apoptotic cell death. In brief, sections of heart tissue were incubated with PI without permeabilization, and then TUNEL staining was performed per the manufacturer's instructions. The nuclei were stained with DAPI and examined using virtual microscopy (BX51/dot slide; Olympus, Tokyo, Japan).

### 4. Cell culture and induction of hypoxia

The rat cardiomyocyte-derived H9c2 cell line (American Type Culture Collection) was cultured in high glucose-DMEM (Gibco, Waltham,

Massachusetts, USA) containing 10% FBS (Atlas Biologicals, Colorado, USA) and 1% antibiotics (Gibco). To induce necroptosis and apoptosis, cells were incubated in a hypoxic chamber (Thermo Fisher Scientific, Massachusetts, USA) maintaining 1% $O_2$, 5% $CO_2$, and 94% $N_2$.

**5. Cell viability assay**

For analysis of cell viability, cells plated or transfected with miRNAs were exposed to hypoxic conditions for 12 h. Then, cell counting kit-8 reagent (CCK-8, Dogen, Seoul, Korea) was added to each well to a final concentration of 0.5 mg/mL, and the cells were incubated for 2 h. The absorbance at 450 nm was measured using a microplate reader (Thermo Fisher Scientific).

**6. Transfection of miRNA and anti-miRNA**

Transfection of miRNA (Genolution Pharmaceuticals, Seoul, Korea) was performed using the TransIT-X2 system (Mirus Bio LLC, Madison, WI, USA) for 12 h. The miRNA-105 sequence is 5'-CAAGUGCUCAGAUGU CUGUGGU-3'. H9c2 cells were transfected with a final concentration of 10 nM miRNA according to the manufacturer's instructions. Anti-miRNA-105 (10 nM) was used to inhibit

the expression of endogenous miRNA-105. After transfection of miRNA or anti-miRNA, the media were changed for stabilization, and then hypoxia was induced.

**7. Real-time RT-PCR**

Total RNA from cultured cells and heart tissues was extracted using TRIzol reagent (Life Technologies, Frederick, MD, USA), and cDNA was synthesized using an RT premix kit (Bioneer Corporation, Daejeon, Korea). The level of each gene transcript was quantitatively determined by qPCR using StepOnePlus real-time PCR (Applied Biosystems, Foster City, CA, USA) with the SYBR Green Dye system (SYBR Premix Ex Taq[(Tli RNase H Plus, ROX plus], Takara Bio Inc., Foster City, CA, USA). The transcript level of each gene was normalized to GAPDH transcript levels. The level of miRNA transcripts was quantitatively determined using reverse transcription (Taqman® MicroRNA Reverse Transcriptase Kit, Applied Biosystems, Waltham, Massachusetts, USA) in combination with Taqman miRNA assays, assays for quantification of miRNAs (miR-105, miR-224, miR-291a) and U6 control transcripts, according to the manufacturer's instructions. The threshold cycle (Ct) value of miRNAs and U6 expression was automatically defined, located in the linear amplification phase

of the PCR, and normalized to the control U6 (ΔCt value). The relative difference in expression level of miRNAs in the sorted cells (ΔΔCt) was calculated and presented as the fold induction ($2^{-\Delta\Delta Ct}$).

## 8. Immunoblot analysis

Cells were lysed with RIPA buffer (Thermo Fisher Scientific) containing 1% phosphatase inhibitor and 1% protease inhibitor. Protein concentrations were determined using the BCA Protein Assay kit (Thermo Fisher Scientific), and 10 μg of protein was diluted in sample buffer (50 mM pH 6.8 Tris, 2% SDS, 10% glycerol, 0.1% bromophenol blue, and 5% β-mercaptoethanol) and heated for 5 min at 99 ℃. Next, proteins were separated by SDS-polyacrylamide gel electrophoresis (PAGE) and transferred to a polyvinylidene difluoride (PVDF; Millipore) membrane. The membrane was blocked for 1 h with 5% skim milk in TBS (Tris-buffered saline)-T buffer (containing 10 mM Tris-HCl, 150 mM NaCl, 0.1% Tween 20) and incubated overnight at 4 ℃ with a primary antibody. Primary antibody was diluted in TBS-T buffer containing 5% BSA (AMRESCO, Solon, Ohio, USA) and 0.02% sodium azide (Sigma-Aldrich). After five washes, the membrane was incubated for 1 h with horseradish peroxidase (HRP)-conjugated anti-mouse IgG, anti-goat IgG, or anti-rabbit IgG (1:2000, Santa Cruz

Biotechnology) in blocking buffer and then washed five times. The membranes were visualized using an enhanced chemiluminescence system (ECL, Western Blotting Detection kit, GE Healthcare), and the band intensities were quantified using ImageJ software.

### 9. Multicolor immunofluorescence staining

For analysis of target protein expression patterns in rat hearts under physiological conditions, perfused hearts were fixed with 4% formaldehyde and embedded in paraffin. Three-micron-thick sections were mounted on gelatin-coated glass slides. After deparaffinization and washing with PBS, sections were incubated in blocking solution containing 2% normal horse serum, 1% BSA, 0.1% Triton X-100, and 0.05% Tween 20 in PBS. Slides were incubated with a mixture of two primary antibodies (RIP3 and p-MLKL) at the appropriate dilutions in PBS containing 1% BSA for 24 h at 4 °C, and FITC-conjugated goat anti-rabbit IgG and rhodamine-conjugated goat anti-mouse were used as secondary antibodies (1:500). The nuclei were stained with DAPI and examined using virtual microscopy (BX51/dot slide; Olympus, Tokyo, Japan).

## 10. Annexin V / PI flow cytometric analysis

Apoptotic or necrotic H9c2 cells were detected using Annexin V and PI staining (BD Biosciences, Franklin Lakes, New Jersey, USA). Annexin V and PI staining were performed according to the manufacturer's instructions. After staining for 15 min, cells were analyzed by flow cytometry (BD ACCURI C6 cytometer, BD Biosciences). Annexin V-/PI+ cells indicated cells undergoing necrotic cell death. Annexin V+/PI- cells indicated cells undergoing early stages of apoptosis. Double-positive cells indicated necrotic cell death and late stages of apoptosis.

## 11. Statistical analysis

All quantified data are the averages of at least triplicate samples. The error bars are the S.D. of the mean. Statistical significance was determined by Student's t test, and values of $P<0.05$ were considered significant.

# III. RESULTS

## 1. Apoptosis and necroptosis of rat hearts following myocardial ischemia and infarction

First, we investigated the types of cell death distributed in the heart after MI (Figure 1). TTC staining revealed that the hearts of healthy rats showed a uniform staining pattern, while MI-induced rats exhibited TTC-negative areas in the infarcted areas of the heart (Figure 1A). We used TUNEL and PI staining to examine the apoptosis and necroptosis levels in the heart following MI (Figure 1B).

Compared with normal hearts, MI hearts showed higher levels of apoptosis and necroptosis. Western blot analysis showed that the levels of indicators of apoptosis (caspase 3, caspase 8, BNIP3) and necroptosis (RIP3, p-MLKL) were significantly increased in hearts after MI (Figure 2A). Moreover, the levels of apoptosis and necroptosis markers significantly increased; the highest level of BNIP3 was indicated at 48 h, while the highest level of RIP3 was observed at 24 h after MI (Figure 2B).

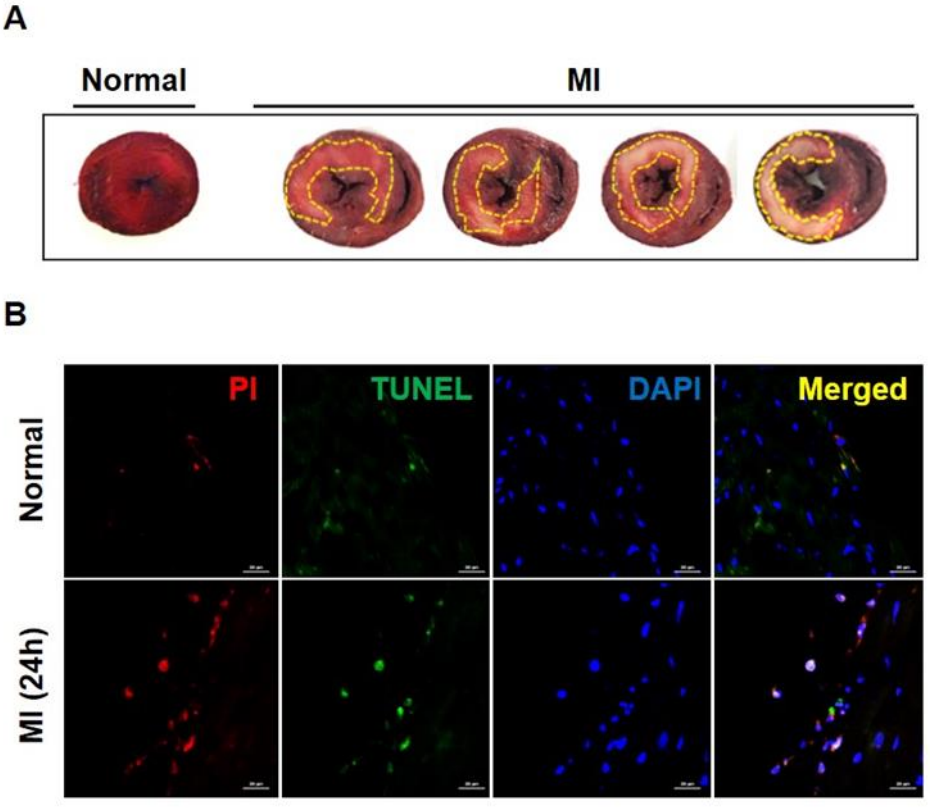


**Figure 1. Apoptotic/necroptotic effects in normal and MI rat hearts**

(A) TTC staining showing infarct areas in transverse sections. (B) Representative immunofluorescence images of staining with TUNEL (apoptotic cells), PI (necroptotic cells), and DAPI. Scale bar = 20 μm.

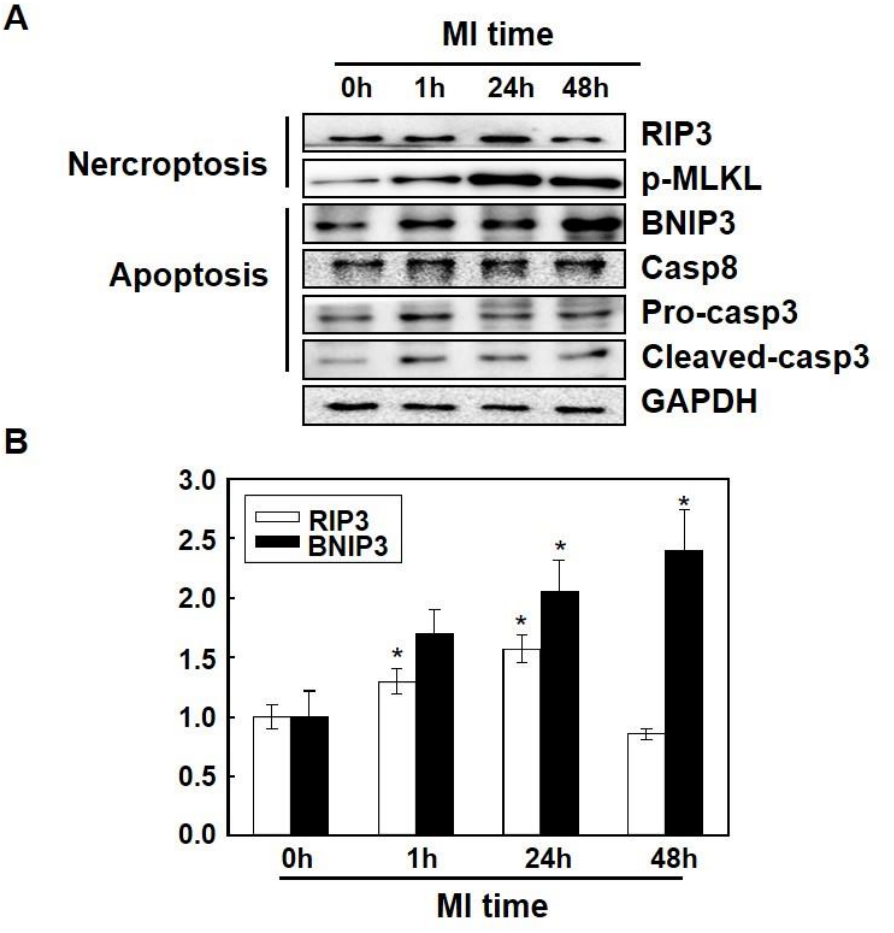


**Figure 2. Differentiation of apoptosis/necroptosis markers in normal and MI of rat heart.**

(A) Western blot bands showing apoptosis and necroptosis markers. (B) Band intensity of RIP3 and BNIP3, which are important markers of apoptosis and necroptosis. Values given were normalized to the band intensity of GAPDH as an internal control. (*$p$<0.05, **$p$<0.01)

These data confirmed that apoptosis and necroptosis occurred in the heart after MI. Microscopic analysis of MI rat hearts showed that apoptosis (BNIP3 and caspase 3) and necroptosis (RIP3 and p-MLKL) markers were found at higher levels in the infarcted areas of MI rat hearts (Figure 3A and 3B).

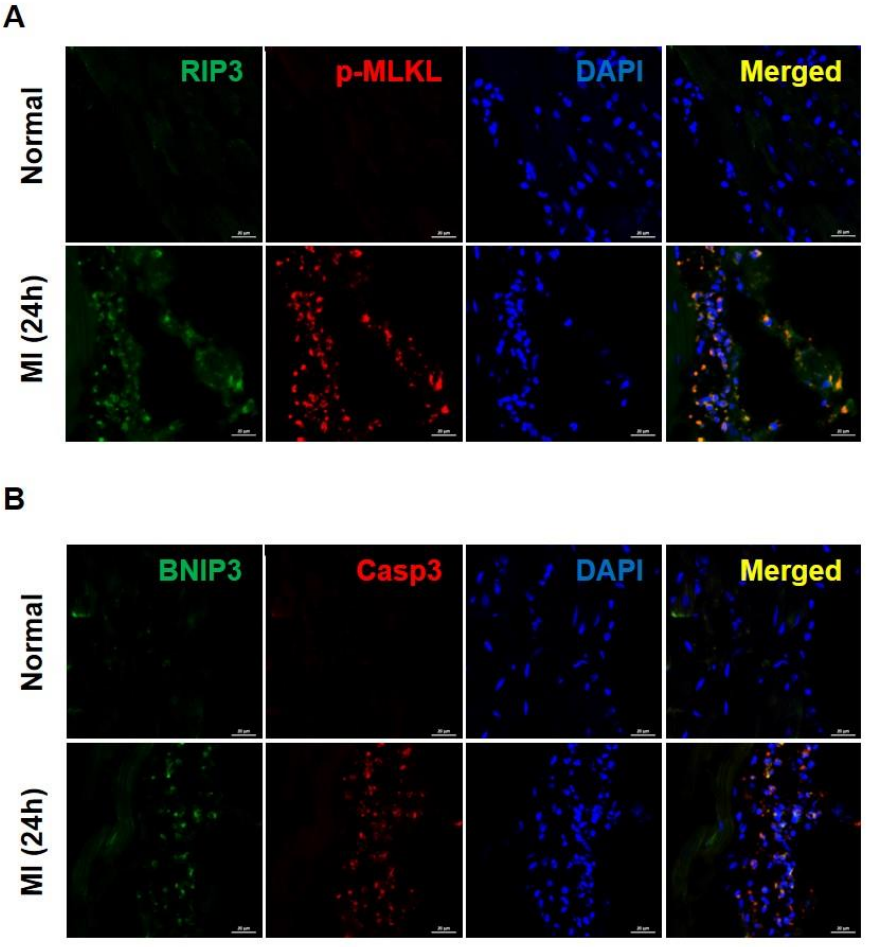


**Figure 3. Representative immunofluorescence images of apoptosis and necroptosis marker staining in normal and MI rat hearts.**

(A) Higher expression of BNIP3 and caspase 3 (CASP3) indicating apoptotic cells in MI tissues. (B) Higher expression of RIP3 and p-MLKL showing necroptotic cells in MI tissues. Scale bar = 20 μm.

## 2. Cell viability and key signaling molecule expression levels under apoptotic/necroptotic conditions

To determine cell viability after hypoxia treatment, H9c2 cell viability was determined after varying times of hypoxia treatment conditions (Figure 4A). There was a significant decrease in cell viability after 6 h, 12 h, 24 h, and 48 h of hypoxia treatment compared to that of the 0 h control sample under normoxic conditions (no hypoxic stimulation). Microscopic analysis of H9c2 cells compared to normoxic cells revealed decreased numbers and different morphology under hypoxic conditions (Figure 4B).

We differentiated between two types of cell death (apoptosis and necroptosis) at the cell level by flow cytometry analysis with Annexin V/propidium iodide (PI) staining (Figure 5). Double negative cells indicate the live cell population, Annexin V-positive/PI-negative events are apoptotic cells (16.1%), double positive events show dead cells (64.8%), and PI-positive/Annexin V-negative events are necroptotic cells (12.5%) after 12 h of hypoxia.

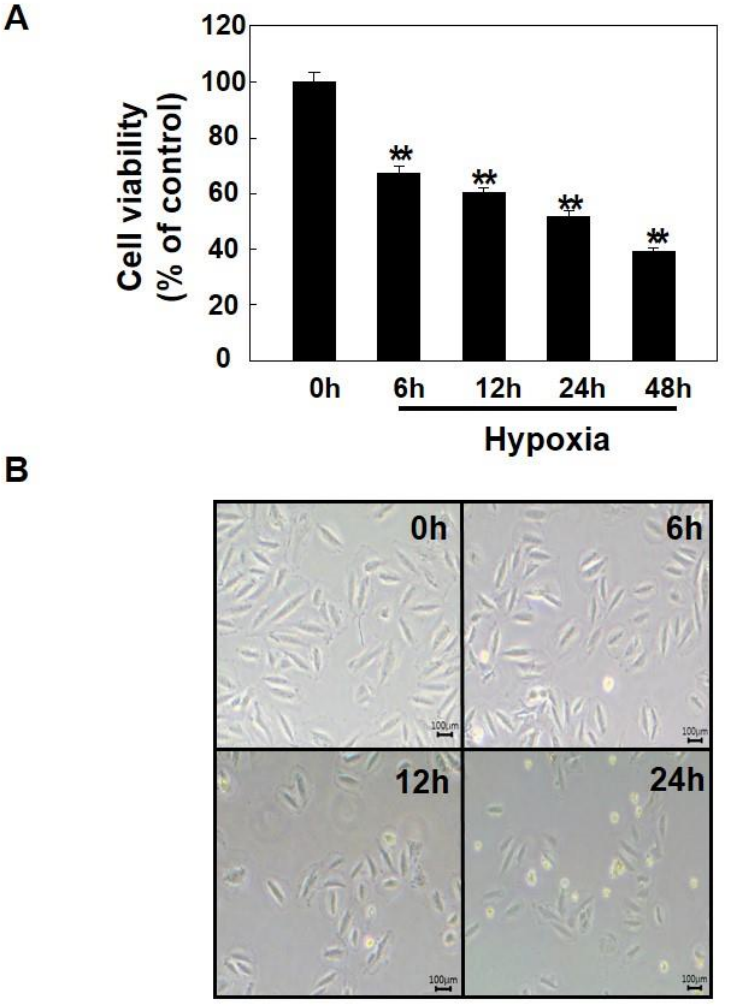


**Figure 4. The effect of hypoxic stimulation on H9c2 cells.**

(A) Cell viability against hypoxic stimulation. (B) Morphological changes according to length of hypoxia. H9c2 cells were treated with no hypoxia under growth conditions of 37 °C in a 5% $CO_2$ incubator or 6 h – 24 h hypoxia under growth conditions of 37 °C, continuously gassed with <1% $O_2$, 5% $CO_2$, and 94% $N_2$. Data are normalized to the 0 h control. Data are presented as the mean value ± STD of three separate experiments.

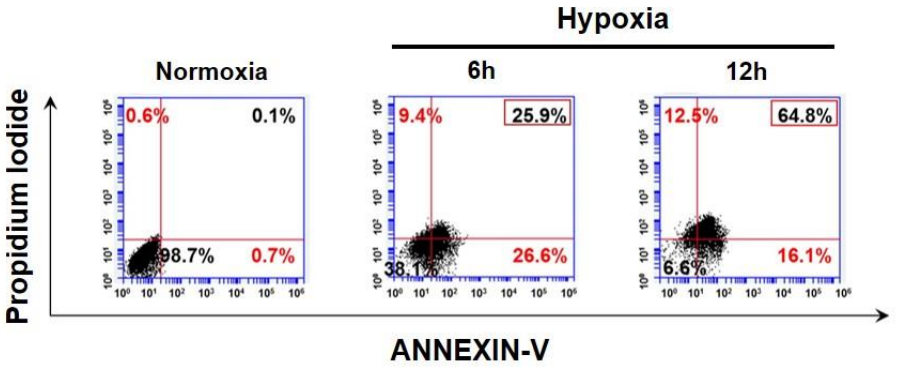


**Figure 5. Flow cytometry analysis of apoptosis/necroptosis of H9c2 cells under hypoxic stimulation using Annexin V/PI.**

To investigate the mRNA expression levels of RIP3 and BNIP3 under hypoxic conditions, H9c2 cells were exposed to varying lengths of hypoxia (0-24 h). Consistent with the MI heart results, the highest RIP3 mRNA level was detected after 12 h of hypoxia, whereas the mRNA levels of BNIP3 increased with the duration of hypoxia (Figure 6).

We further investigated the relative changes of protein indicators of apoptosis (BNIP3, BAK, BAX, caspase 3) and necroptosis (RIP3, p-MLKL) under hypoxia (Figure 7A and B). Consistent with the mRNA expression levels, the results of the western blot showed that apoptosis and necroptosis significantly increased after hypoxia and reached a maximum at 24 h and 12 h of hypoxia. Collectively, the results demonstrated that hypoxia induced apoptosis and necroptosis in H9c2 cells *in vitro*. Moreover, we examined whether cardiac Toll-like receptor 4 (TLR4) and tumor necrosis factor receptor 1 (TNFR1) are involved in hypoxia-treated H9c2 cells. The expression levels of the two receptors were increased after hypoxic treatment; the highest level of receptors was detected after 12 h of hypoxia in H9c2 cells.

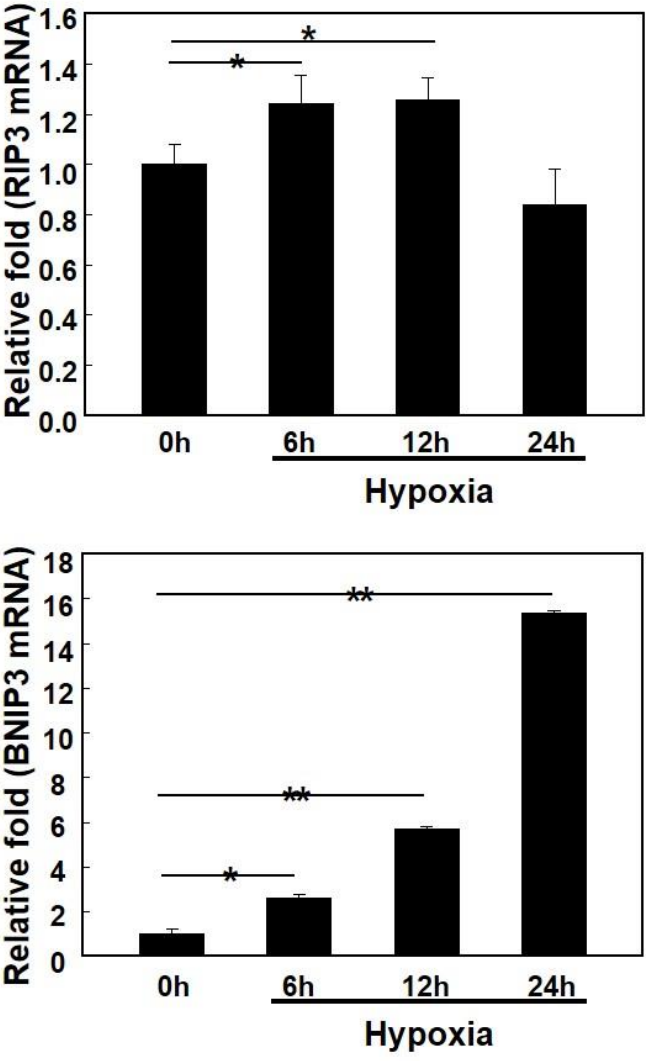


**Figure 6. Alteration of RIP3 and BNIP3 expression levels in response to hypoxic stimulation in H9c2 cells.**

Data are normalized to the 0 h control. Data are presented as the mean value ± STD of three separate experiments. (*$p$<0.05, **$p$<0.01)

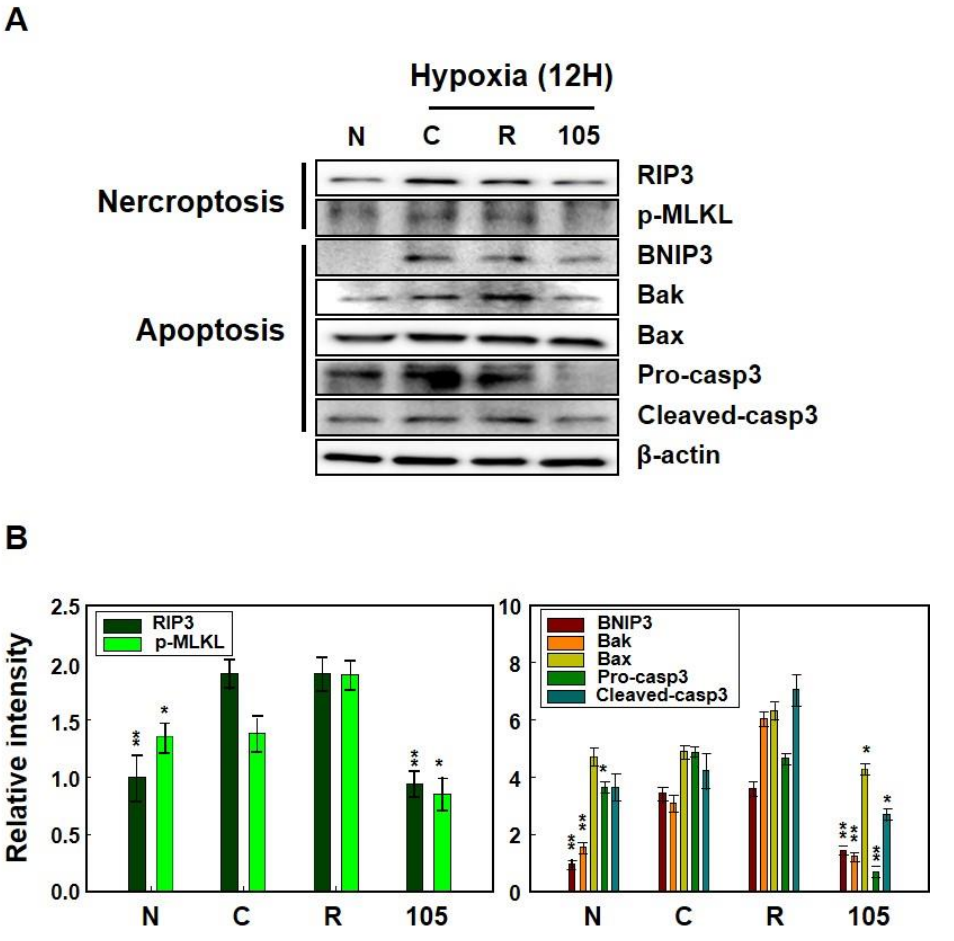


**Figure 7. Differentiation of apoptosis/necroptosis markers and death receptors in response to hypoxic stimulation.**

(A) Western blot bands showing apoptosis and necroptosis markers. (B) Band intensity of apoptosis and necroptosis markers. Values given were normalized to the band intensity of β-actin as an internal control. (*$p$<0.05, **$p$<0.01)

BNIP3/CASP3 and RIP3/p-MLKL are widely used indicators to mark the cell death pathways of apoptosis and necroptosis, respectively. By immunohistochemical analysis, BNIP3/CASP3- and RIP3/p-MLKL-positive cells significantly increased after 12 h of hypoxia in H9c2 cells (Figure 8A and B). Many more cardiomyocytes undergoing apoptotic/necroptotic cell death appeared in hypoxia-treated cells than those in H9c2 cells in normoxic conditions.

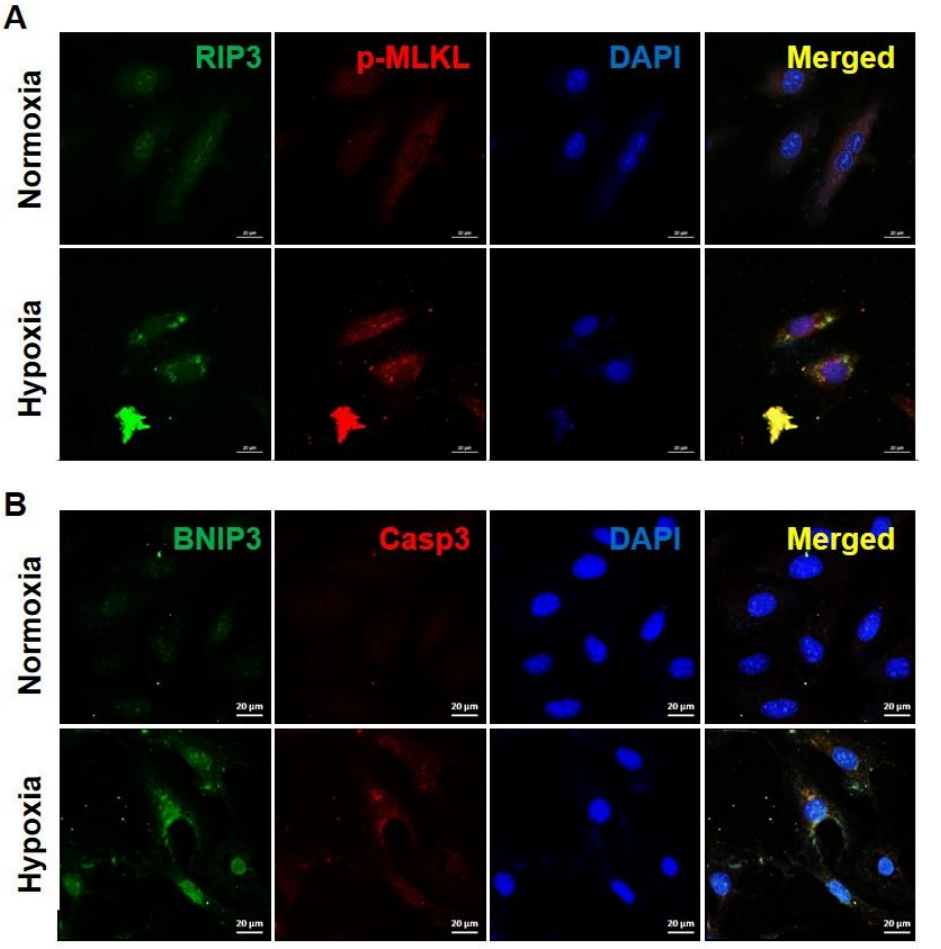


**Figure 8. Representative immunocytochemistry images of apoptosis/necroptosis markers in response to hypoxic stimulation of H9c2 cells.**

(A) Higher expression of BNIP3 and caspase 3 (CASP3) showing apoptotic cells in hypoxia-treated H9c2 cells. (B) Higher expression of RIP3 and p-MLKL showing necroptotic cells in hypoxia-treated H9c2 cells. Scale bar = 20 μm.

### 3. Identification of a specific miRNA targeting RIP3/BNIP3

Candidate miRNAs (miR-105, miR-224, miR-291a) controlling the multiple programmed cell death pathways were predicted and selected by their aggregate PCT scores, as assessed using miRNA target prediction databases (miRwalk, miRanda, TargetScan) (Figure 9).

H9c2 cells transfected with miR-105 and 291a showed significant decreases in both RIP3 and BNIP3 protein expression levels compared to the control, while miR-224 showed no effects after 12 h of hypoxic conditions (Figure 10).

In correlation with the decreased RIP3 and BNIP3 protein expression levels, the highest cell viability was observed after 12 h of hypoxia in H9c2 cells transfected with miR-105 (Figure 11).

| Target | miRNA target prediction data base | | |
|---|---|---|---|
| | miRwalk | miRanda | Targetscan |
| **RIP3** | miR-20b miR-223 **miR-224 miR-105** miR-106b **miR-291a** miR-3085 miR-17 miR-3102 miR-93 | | |
| **BNIP3** | miR-3588 miR-9b miR-190b miR411 miR-3120 miR-764 **miR-291a** miR-449c miR-153 miR-3594 miR-336 miR29a miR-let-7f-2 miR-873 miR-29b-1 miR-374 miR-673 miR-182 **miR-224** miR-674 miR-186 **miR-105** miR-137 miR-702 miR-3068 miR-742 miR-26a miR-6333 miR-142 miR-206 | | |

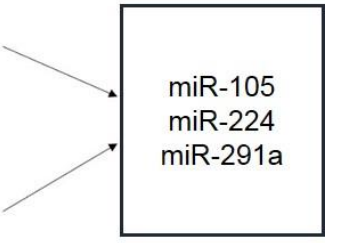


**Figure 9. Identification of specific miRNAs targeting RIP3 and BNIP3.**

Candidate miRNAs were found using three databases (TargetScan, miRwalk, miRanda).

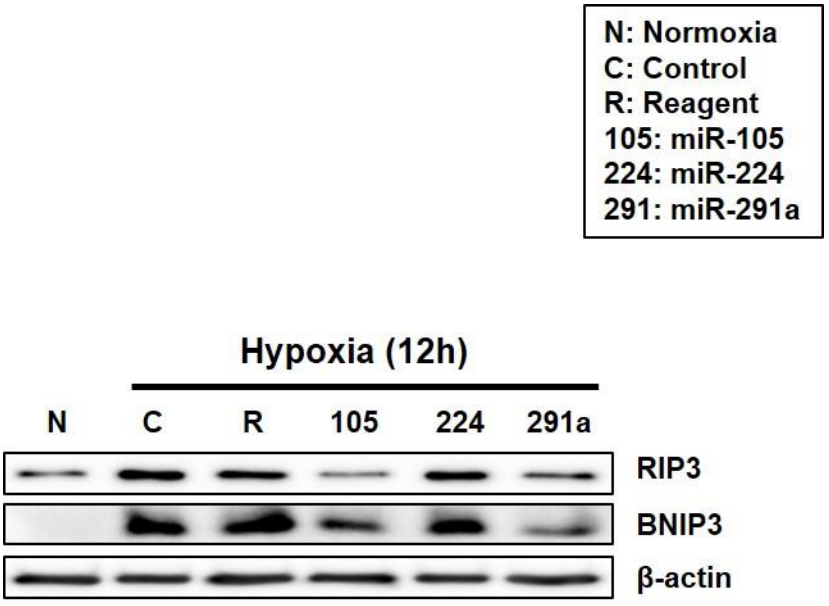


**Figure 10. Anti-apoptotic/necroptotic effects of candidate miRNAs on RIP3 and BNIP3 expression levels upon hypoxic stimulation of H9c2 cells.**

β-actin was used as an internal control to normalize the expression of the target genes.

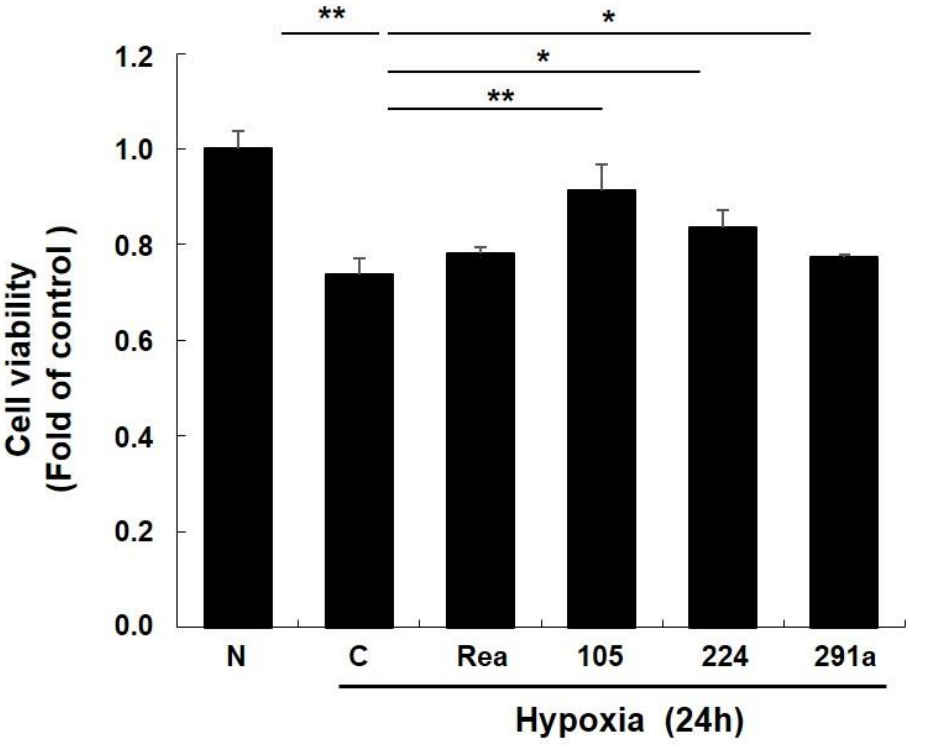


**Figure 11. Enhancing cell viability with candidate miRNA transfection upon hypoxic stimulation of H9c2 cells.**

Data are presented as the mean value ± STD of three separate experiments. (*$p$<0.05, **$p$<0.01)

### 4. MicroRNA-105 suppresses necroptosis/apoptosis in hypoxia-treated H9c2 cells

To examine the role of miR-105 in the regulation of apoptosis and necroptosis, cell cytotoxicity was examined in hypoxia-treated H9c2 cells; miR-105 treatment suppressed BNIP3/RIP3 in the cells (Figure 12). As depicted in Figure 13, miR-105 downregulated apoptosis indicators, such as BNIP3, and necroptosis markers, such as RIP3.

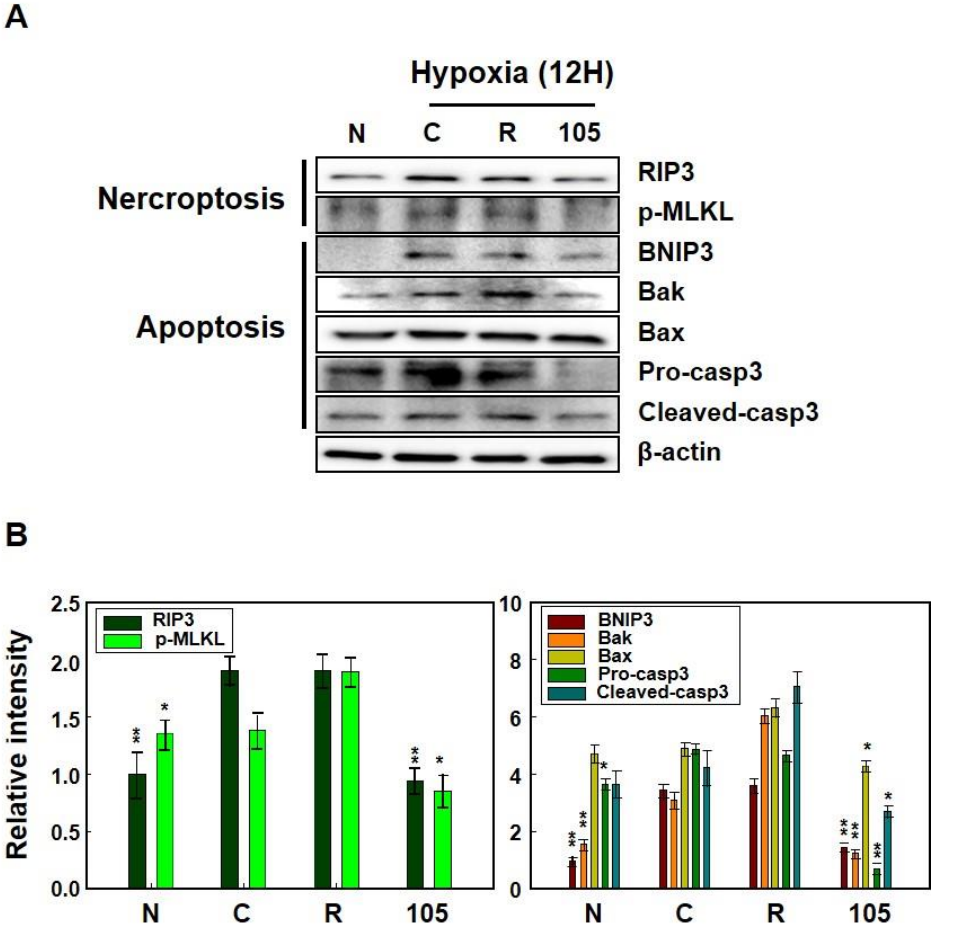


**Figure 12. miR-105 suppresses apoptosis and necroptosis against hypoxic stimulation of H9c2 cells.**

(A) Representative western blot bands showing apoptosis and necroptosis markers. (B) Band intensity of apoptosis and necroptosis markers. Values given were normalized to the band intensity of β-actin as an internal control. (*$p$<0.05, **$p$<0.01)

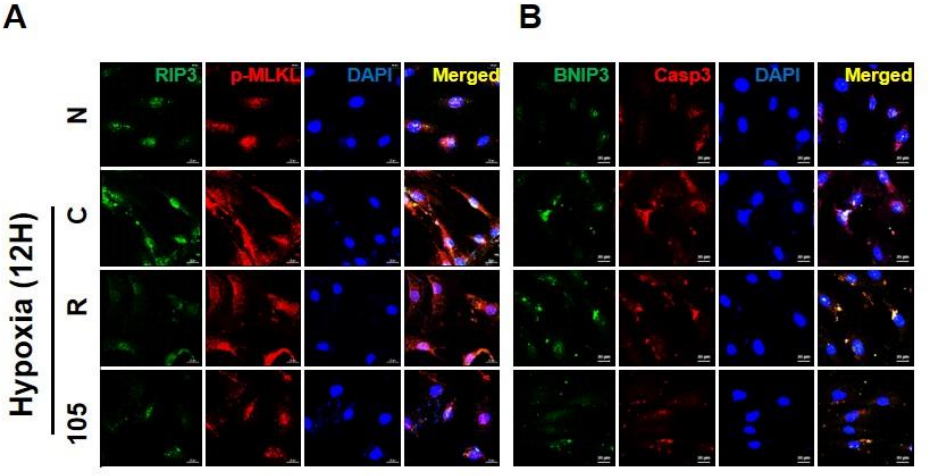


**Figure 13. Representative immunocytochemistry images of miR-105 suppression effects on apoptosis and necroptosis upon hypoxic stimulation of H9c2 cells.**

(A) Higher expression of BNIP3 and caspase 3 (CASP3) showing apoptotic cells in hypoxia-stimulated H9c2 cells, whereas expression was downregulated by miR-105. (B) Higher expression of RIP3 and p-MLKL showing necroptotic cells in hypoxia-stimulated H9c2 cells, whereas expression was downregulated by miR-105. Scale bar = 20 μm.

Next, to determine whether transfection affects cell viability, we examined two types of cell death (apoptosis and necroptosis) by flow cytometry analysis with Annexin V/PI staining under hypoxic conditions (Figure 14). Annexin V-positive/PI-negative events indicate apoptotic cells (16.4%), double positive events show dead cells (35.4%) and PI-positive/Annexin V-negative events indicate necroptotic cells (12.1%) after 12 h of hypoxia. As expected, miR-105-transfected H9c2 cells had enhanced cell viability against hypoxia-induced apoptosis/necroptosis. The number of apoptotic and necroptotic cells was markedly decreased in the presence of miR-105. Moreover, in accordance with our *in vitro* experiments under hypoxic conditions, we confirmed that miR-105 was significantly downregulated in MI rat hearts.

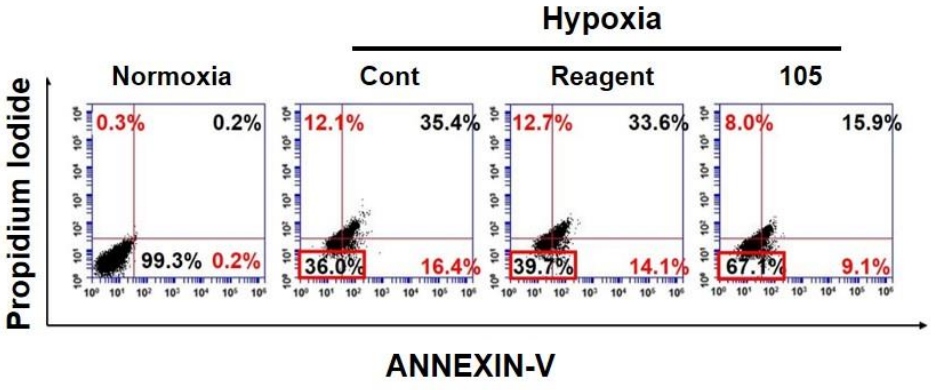


**Figure 14. Anti-necroptotic/apoptotic effects of miR-105 under hypoxic conditions in H9c2 cells by flow cytometry analysis using Annexin V/PI.**

## 5. Anti-necroptosis/apoptosis functions of miR-105 in hypoxia-treated H9c2 cells

To evaluate the relative contributions of necroptosis/apoptosis to hypoxia-induced cell death, we used a CCK assay, which measures both apoptotic and necroptotic cell death, in the presence or absence of the pan-caspase inhibitor zVAD, the RIP3 inhibitor GSK'872, and anti-miR-105 (Figure 15A). Hypoxia-induced cell death could not be blocked by zVAD or GSK'872 alone, suggesting that under the conditions used, hypoxia-induced cardiomyocyte death is mediated by both cell death pathways. Notably, miR-105-transfected cells exhibited the highest cell survival efficiency as in the zVAD/GSK'872 combined treatment. Moreover, cleaved caspase 3 and RIP3 expression decreased more in miR-105-transfected cells compared with that in the combined zVAD/GSK'872 treatment (Figure 15B). We next determined the functional role of miR-105 with anti-miR-105 against hypoxic stimulation in H9c2 cells (Figure 15C).

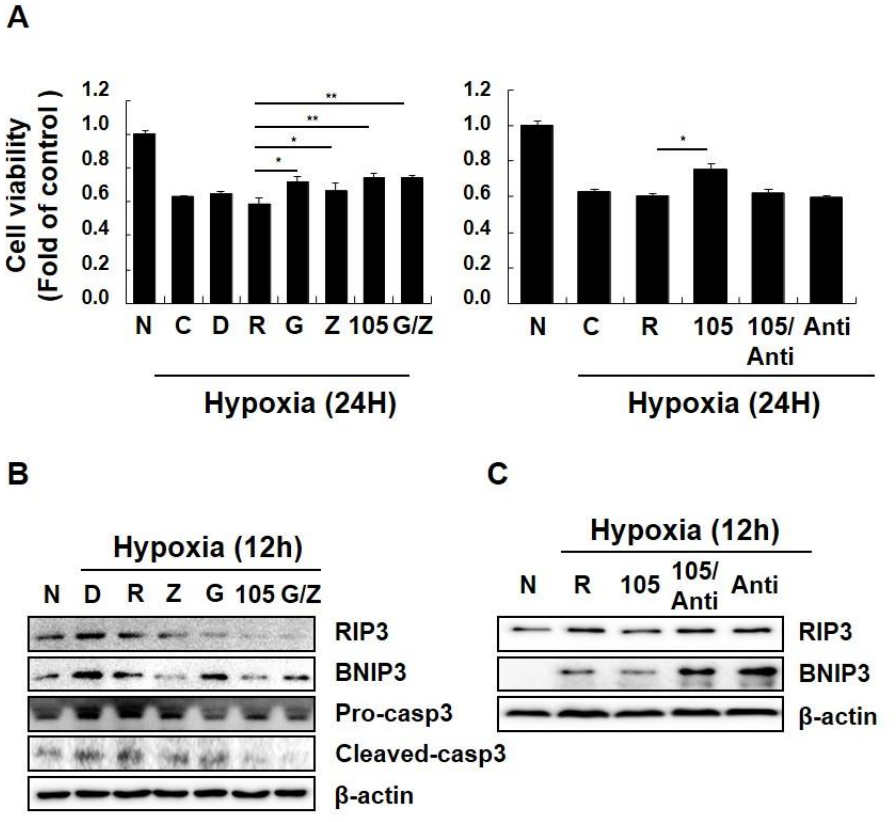


**Figure 15. Anti-necroptotic/apoptotic functions of miR-105 in hypoxia-stimulated H9c2 cells.**

(A) Effects of cell viability by inhibitor and anti-miR-105. (B) Effect of necroptosis/apoptosis inhibitors and miR-105 against hypoxic stimulation in H9c2 cells. Verification of the efficacy and specificity of anti-miR-105 in silencing miR-105 at the protein level. ± STD of five separate experiments. (*$p$<0.05, **$p$<0.01) C, control; D, DMSO; R, reagent; Z, Caspase inhibitor; G, RIP3 inhibitor; 105, miR-105; anti, anti-miR-105.

## 6. MicroRNA-105 suppresses necroptosis/apoptosis in MI rat hearts

First, we confirmed the higher expression of miR-105 in MI rat hearts compared with that in control hearts (Figure 16). We determined the functional role of miR-105 in infarcted hearts and found that miR-105 significantly reduced the infarct size in MI (Data not shown). We tried to clarify whether the anti-necroptosis/apoptosis effects of miR-105 observed in H9c2 cells under hypoxic conditions also exist in *in vivo* in MI rat hearts. In agreement with the *in vitro* results, TUNEL and PI staining analysis showed that cardiomyocyte necroptotic/apoptotic cell death induced by MI was markedly reduced in miR-105-treated rat hearts (Figure 17).

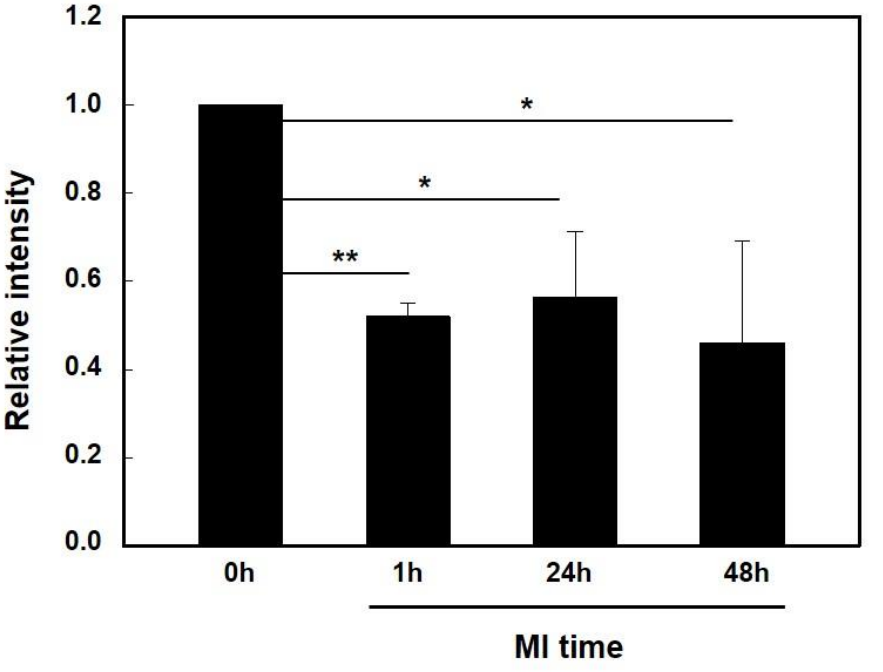


**Figure 16. miR-105 suppresses apoptosis and necroptosis in MI rat hearts.**

miR-105 expression levels according to MI time. Data are normalized to the 0 h control. Data are presented as the mean value ± STD of three separate experiments. (*$p$<0.05, **$p$<0.01)

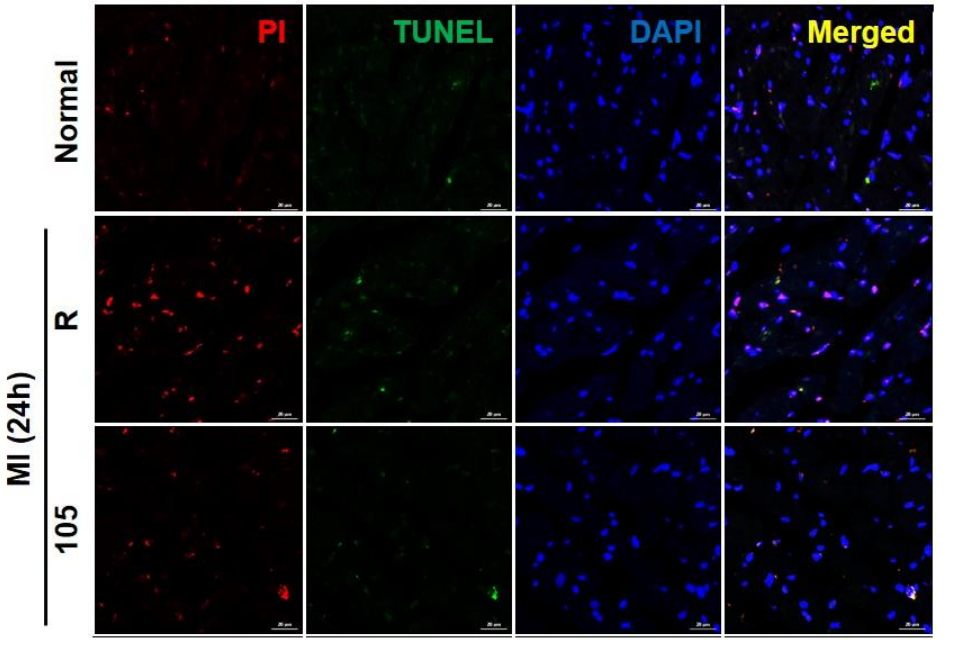


**Figure 17. Regulatory effects of miR-105 on apoptotic and necroptotic action in MI rat hearts.**

Representative immunofluorescence images of staining with TUNEL (apoptotic cells), PI (necroptotic cells), and DAPI. Scale bar = 20 μm.

MI rat heart tissue showed significantly increased cardiomyocyte necroptosis/apoptosis, and treatment with miR-105, whether individually, drastically decreased this ischemic necroptosis/apoptosis compared with that in MI rat hearts. Furthermore, western blot data showed that, compared to control MI rat hearts, MI rat hearts transfected with miR-105 showed a significant decrease in both RIP3 and BNIP3 protein expression levels (Figure 18). In conclusion, miR-105 synergistically inhibits RIP3 and BNIP3 against myocardial cell death.

Based on these *in vivo* and *in vitro* data, we conclude that both cardiomyocyte necroptosis and apoptosis have important roles in hypoxia-induced myocardial injury. miR-105 functions to simultaneously suppress necroptotic/apoptotic cell death pathways and cooperatively inhibit MI-induced cardiomyocyte cell death.

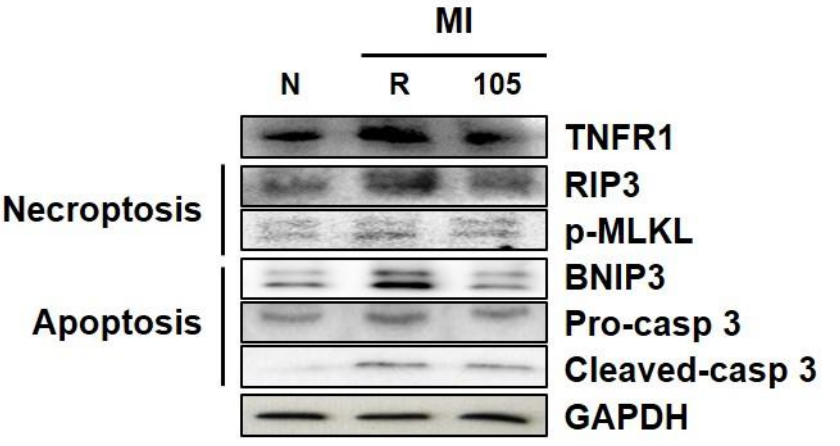


**Figure 18. Anti-necroptotic/apoptotic functions of miR-105 in MI rat hearts.** Representative western blot images of RIP3 and BNIP3 expression levels. GAPDH was used as an internal control to normalize the expression of the target genes. N, normal; R, reagent; 105; miR-105.

## IV. DISCUSSION

In this study, we observed that miR-105, which targets RIP3/BNIP3, was notably dysregulated in rat hearts with MI. The purpose of this study was to test the hypothesis of whether miR-105 participates in the regulation of RIP3/p-MLKL- and BNIP3-dependent cell death pathways, necroptosis and apoptosis, in H9c2 cells and MI rat hearts.

miRNAs play important roles in regulating myocardial injuries and cardiac functions in the setting of acute MI (AMI) [26-28]. Furthermore, miRNAs play important roles in pathological conditions involving apoptosis, including AMI and heart failure [29]. For many years, apoptosis was considered the only form of regulated cell death, and studies investigating MI mainly focused on apoptosis [5]. In recent years, necroptosis has been described as another regulated cell death form that exists in various diseases, including MI [30]. However, whether all cell death mechanisms in MI affect subsequent cardiac remodeling processes remains largely unknown.

A recent study reported that the combination of two miRNAs (miR-21 and miR-146a) synergistically decreased apoptosis under ischemic/hypoxic conditions in acute MI in mice [26]. Among the cell death pathway-regulating

miRNAs, both miR-21 and miR-146a have been documented to elicit anti-apoptotic effects and thereby beneficial effects on ischemic myocardial injury [26]. As further evidence, miR-98 overexpression attenuated the upregulation of Fas and caspase 3 in H2O2-treated cardiomyocytes at the mRNA and protein levels [31]. Furthermore, MI mice injected with miR-98-agomir had a significant reduction in the number of apoptotic cells, serum LDH levels, myocardial caspase 3 activity, and Fas and caspase 3 expression in heart tissues. However, for the first time, our study confirmed that miR-105, which targets RIP3/BNIP3, simultaneously dysregulates necroptotic and apoptotic cell death in rat MI hearts and H9c2 cells under hypoxic conditions. We identified the signaling pathway responsible for the anti-necroptotic/apoptotic effects of miR-105 against hypoxia-induced myocardial injury *in vivo* and *in vitro.*

A large amount of evidence has placed RIP3/MLKL and BNIP3/caspase 3 in a central position in the pathogenesis of ischemia- and oxidative stress-induced cardiac injury and heart failure [26, 30-32]. For many years, apoptosis was considered the only form of regulated cell death, and studies investigating MI mainly focused on apoptosis [33, 34]. In recent years, necroptosis has been found to be another regulated cell death type existing in various diseases including MI [35-37]; however, few studies have focused on necroptosis in MI [30]. However, whether all

mechanisms of cell death in MI affect the subsequent cardiac repair process remains largely unknown. In this study, we observed that cardiomyocyte cell death upon hypoxic treatment was attenuated dramatically when treated with GSK'872 (a RIP3 inhibitor) or zVAD (a caspase inhibitor). Moreover, miR-105 significantly ameliorated cell injury and attenuated cell death as did the combined zVAD/GSK'872 treatment against hypoxic conditions in cardiomyocytes. In agreement with the *in vitro* results, we found that miR-105 functions to simultaneously suppress BNIP3/RIP3 expression levels, which are the primary mediators of necroptotic/apoptotic cell death pathways in MI rat hearts.

## V. CONCLUSION

The current study shows that the distribution of apoptosis and necroptosis differs in a time-dependent manner after MI or hypoxia stimulation. Moreover, miR-105 treatment improves the cell viability of H9c2 cells by inhibiting apoptosis and necroptosis, which is associated with the regulation of the interplay between them. Thus, our results offer strategies for the treatment of MI and post-MI cardiac remodeling.

## REFERENCES

1. Morys JM, Bellwon J, Hofer S, Rynkiewicz A, Gruchala M. Quality of life in patients with coronary heart disease after myocardial infarction and with ischemic heart failure. Archives of medical science. 2016; 12: 326-33.
2. Sulo G, Igland J, Vollset SE, Nygard O, Tell GS, et al. Heart Failure Complicating Acute Myocardial Infarction; Burden and Timing of Occurrence: A Nation-wide Analysis Including 86 771 Patients From the Cardiovascular Disease in Norway (CVDNOR) Project. Journal of the American Heart Association. 2016; 5.
3. Rahimi K, Duncan M, Pitcher A, Emdin CA, Goldacre MJ. Mortality from heart failure, acute myocardial infarction and other ischaemic heart disease in England and Oxford:a trend study of multiple-cause-coded death certification. Journal of epidemiology and community health. 2015; 69: 1000-5.
4. Ho JE, Bittner V, Demicco DA, Breazna A, Waters DD, et al. Usefulness of heart rate at rest as a predictor of mortality, hospitalization for heart failure, myocardial infarction, and stroke in patients with stable coronary heart disease (Data from the Treating to New Targets [TNT] trial). The American journal of cardiology. 2010; 105: 905-11.

5. Whelan RS, Kaplinskiy V, Kitsis RN. Cell death in the pathogenesis of heart disease: mechanisms and significance. Annual review of physiology. 2010; 72: 19-44.
6. de Zwaan C, Daemen MJ, Hermens WT. Mechanisms of cell death in acute myocardial infarction: pathophysiological implications for treatment. Netherlands heart journal : monthly journal of the Netherlands Society of Cardiology and the Netherlands Heart Foundation. 2001; 9: 30-44.
7. Oerlemans MI, Koudstaal S, Chamuleau SA, de Kleijn DP, Sluijter JP et al. Targeting cell death in the reperfused heart: pharmacological approaches for cardioprotection. International journal of cardiology. 2013; 165: 410-22.
8. Weinlich R, Oberst A, Beere HM, Green DR. Necroptosis in development, inflammation and disease. Nature reviews Molecular cell biology. 2017; 18: 127-36.
9. Linkermann A, Green DR. Necroptosis. The New England journal of medicine. 2014; 370: 455-65.
10. Pasparakis M, Vandenabeele P. Necroptosis and its role in inflammation. Nature. 2015; 517: 311-20.
11. Vanden Berghe T, Linkermann A, Jouan-Lanhouet S, Walczak H, Vandenabeele P. Regulated necrosis: the expanding network of non-apoptotic

cell death pathways. Nature reviews Molecular cell biology. 2014; 15: 135-47.

12. Zhou W, Yuan J. Necroptosis in health and diseases. Seminars in cell & developmental biology. 2014; 35: 14-23.
13. Zhang T, Zhang Y, Cui M, Jin L, Xiao RP, et al. CaMKII is a RIP3 substrate mediating ischemia- and oxidative stress-induced myocardial necroptosis. Nature medicine. 2016; 22: 175-82.
14. Kung G, Konstantinidis K, Kitsis RN. Programmed necrosis, not apoptosis, in the heart. Circulation research. 2011; 108: 1017-36.
15. Liang W, Chen M, Zheng D, He J, Lan J, et al. A novel damage mechanism: Contribution of the interaction between necroptosis and ROS to high glucose-induced injury and inflammation in H9c2 cardiac cells. International journal of molecular medicine. 2017; 40: 201-8.
16. Diwan A, Krenz M, Syed FM, Wansapura J, Dorn GW et al. Inhibition of ischemic cardiomyocyte apoptosis through targeted ablation of Bnip3 restrains postinfarction remodeling in mice. The Journal of clinical investigation. 2007; 117: 2825-33.
17. Hamacher-Brady A, Brady NR, Logue SE, Sayen MR, Gustafsson AB, et al. Response to myocardial ischemia/reperfusion injury involves Bnip3 and

autophagy. Cell death and differentiation. 2007; 14: 146-57.

18. Kim JY, Kim YJ, Lee S, Park JH. BNip3 is a mediator of TNF-induced necrotic cell death. Apoptosis : an international journal on programmed cell death. 2011; 16: 114-26.
19. Jain MV, Paczulla AM, Klonisch T, Dimgba FN, Los M., et al. Interconnections between apoptotic, autophagic and necrotic pathways: implications for cancer therapy development. Journal of cellular and molecular medicine. 2013; 17: 12-29.
20. Fordjour PA, Wang L, Gao H, Li L, Fan G, et al. Targeting BNIP3 in inflammation-mediated heart failure: a novel concept in heart failure therapy. Heart failure reviews. 2016; 21: 489-97.
21. Lee SY, Lee S, Choi E, Ham O, Hwang KC, et al. Small molecule-mediated up-regulation of microRNA targeting a key cell death modulator BNIP3 improves cardiac function following ischemic injury. Scientific reports. 2016; 6: 23472.
22. Koshinuma S, Miyamae M, Kaneda K, Kotani J, Figueredo VM. Combination of necroptosis and apoptosis inhibition enhances cardioprotection against myocardial ischemia-reperfusion injury. Journal of anesthesia. 2014; 28: 235-41.

23. Xiaoyun Guo HY, Lei Li, Yi Chen, Jing Li, Qinghang Liu, et al. Cardioprotective Role of TRAF2 by Suppressing Apoptosis and Necroptosis. Circulation. 2017; 136.
24. Bartel DP. MicroRNAs. Cell. 2004; 116: 281-97.
25. Zhenyi Su ZY, Yongqing Xu, Yongbin Chen, Qiang Yu. MicroRNAs in apoptosis, autophagy and necroptosis. Oncotarget. 2015 Apr 20; 6: 8474–90.
26. Huang W, Tian SS, Hang PZ, Sun C, Guo J, Du ZM. Combination of microRNA-21 and microRNA-146a Attenuates Cardiac Dysfunction and Apoptosis During Acute Myocardial Infarction in Mice. Molecular therapy Nucleic acids. 2016; 5: e296.
27. Wang J, Yang X. The function of miRNA in cardiac hypertrophy. Cellular and molecular life sciences : 2012; 69: 3561-70.
28. Chistiakov DA, Orekhov AN, Bobryshev YV. Cardiac-specific miRNA in cardiogenesis, heart function, and cardiac pathology (with focus on myocardial infarction). Journal of molecular and cellular cardiology. 2016; 94: 107-21.
29. Li P. MicroRNAs in cardiac apoptosis. Journal of cardiovascular translational research. 2010; 3: 219-24.
30. Luedde M, Lutz M, Carter N, Sosna J, Frey N, et al. RIP3, a kinase promoting

necroptotic cell death, mediates adverse remodelling after myocardial infarction. Cardiovascular research. 2014; 103: 206-16.

31. Sun C, Liu H, Guo J, Yu Y, Du Z, et al. MicroRNA-98 negatively regulates myocardial infarction-induced apoptosis by down-regulating Fas and caspase-3. Scientific reports. 2017; 7: 7460.
32. Shen C, Wang C, Han S, Wang Z, Dong Z, Sun A et al. Aldehyde dehydrogenase 2 deficiency negates chronic low-to-moderate alcohol consumption-induced cardioprotecion possibly via ROS-dependent apoptosis and RIP1/RIP3/MLKL-mediated necroptosis. Biochimica et biophysica acta. 2017; 1863: 1912-8.
33. Foglio E, Puddighinu G, Germani A, Russo MA, Limana F. HMGB1 Inhibits Apoptosis Following MI and Induces Autophagy via mTORC1 Inhibition. Journal of cellular physiology. 2017; 232: 1135-43.
34. Tao Z, Chen B, Tan X, Zhao Y, Su H. Coexpression of VEGF and angiopoietin-1 promotes angiogenesis and cardiomyocyte proliferation reduces apoptosis in porcine myocardial infarction (MI) heart. Proceedings of the National Academy of Sciences of the United States of America. 2011; 108: 2064-9.
35. Pietkiewicz S, Eils R, Krammer PH, Giese N, Lavrik IN. Combinatorial

treatment of CD95L and gemcitabine in pancreatic cancer cells induces apoptotic and RIP1-mediated necroptotic cell death network. Experimental cell research. 2015; 339: 1-9.

36. Schenk B, Fulda S. Reactive oxygen species regulate Smac mimetic/TNFalpha-induced necroptotic signaling and cell death. Oncogene. 2015; 34: 5796-806.
37. Singla S, Sysol JR, Dille B, Jones N, Machado RF, et al. Hemin Causes Lung Microvascular Endothelial Barrier Dysfunction by Necroptotic Cell Death. American journal of respiratory cell and molecular biology. 2017; 57: 307-14.

## ABSTRACT (IN KOREAN)

# 심근 허혈성 손상에서 miRNA-105에 의한 세포 사멸 억제

< 지도교수 한 균 희 >

연세대학교 대학원 융합오믹스 의생명과학과

신 선 혜

프로그램화 세포사멸인 세포자살 (apoptosis)과 프로그램화 되지 않은 세포사멸인 세포괴사 (necrosis)는 심근경색에 의해서 발생되는데, 최근 프로그램화 세포괴사인 necroptosis 도 심근경색에 의해 발생된다는 것이 밝혀졌다. 본 연구에서는 심근경색에서 발생하는 apoptosis 와 necroptosis 를 동시에 억제할 수 있는 microRNA (miRNA)를 찾고자 하였다.

Receptor-interacting protein kinase 3 (RIP3)는 necroptotis 를 유발하는 주요인자이며, BCL2/adenovirus E1B 19 kDa protein-interacting protein 3 (BNIP3)는 미토콘드리아의 장애를 유발하여 세포 내의 apoptosis 를 조절하는 인자로서 심근경색에 의한 심근세포의 사멸을 확인하는데 유용하다. 따라서 본 연구에서는 저산소 환경의 심근세포 (H9c2) 와 심근경색 동물모델에서 RIP3와 BNIP3의 발현을 조사하였고, 그 결과, 두 인자 모두 시간에 따라 증가하는 것을

확인하였다. 이렇게 확립된 *in vitro* 와 *in vivo* 모델에서 RIP3와 BNIP3를 억제할 것으로 예상되는 후보 miRNA 를 각각 처리한 후, 두 인자의 발현을 조사하였고, 그 결과, miRNA-105를 과발현 시킨 심근세포가 저산소 환경에서 RIP3와 BNIP3를 억제하는 동시에 심근세포의 생존율을 증가시킨다는 것을 확인하였다. 또한 심근경색 동물모델에서 miRNA-105 발현이 감소되어 있었으며, miRNA-105를 주입한 모델의 경우 심장의 손상부위가 감소하였고 세포의 apoptosis 와 necroptosis 가 억제되는 것을 확인하였다. miRNA-105가 심근경색의 apoptosis 와 necroptosis 를 동시에 억제한다는 것은 본 연구에서 최초로 밝힌 것이며, 이러한 결과는 심근경색 치료에 있어서 miRNA-105가 새로운 치료법으로 활용 가능함을 암시하는 것이다.

---

중심어: 세포사멸, 심근경색, microRNA-105, necroptosis,